Electrochemical and Solid-State Letters, **11** (2) P1-P4 (2008)
1099-0062/2007/11(2)/P1/4/$23.00 © The Electrochemical Society

Temperature-Dependent Photoluminescence in $NaTaO_3$ with Different Crystalline Structures

Yueh-Chien Lee,[a,z] Hsisheng Teng,[b,*] Che-Chia Hu,[b] and Sheng-Yao Hu[c]

[a]*Department of Electronic Engineering and Research Center for Micro/Nano Technology, Tungnan University, Taipei 22202, Taiwan*
[b]*Department of Chemical Engineering, National Cheng Kung University, Tainan 70101, Taiwan*
[c]*Department of Electrical Engineering and VLSI/CAD Center, Tung Fang Institute of Technology, Humei Township, Kaohsiung County 82941, Taiwan*

The optical properties of the perovskite-type $NaTaO_3$ synthesized from sol-gel (SG) and solid-state (SS) methods were studied by absorption and photoluminescence (PL) techniques. We observed significant PL emission at room temperature from the SS $NaTaO_3$, while the emission was negligible from the SG $NaTaO_3$. Variation of the PL intensity and peak position with temperature demonstrated that the recombination of the localized exciton Ta^{4+}–O^- in the regular TaO_6 octahedra was the origin of the luminescence in $NaTaO_3$. The Ta–O–Ta bond angle affected the delocalization of the excitons and thus, the PL behaviors of $NaTaO_3$.
 [DOI: 10.1149/1.2817476]

Manuscript submitted September 10, 2007; revised manuscript received October 30, 2007.
Available electronically December 10, 2007.

ABO_3 perovskite structures, where A is a group of I-II elements and B is a transition metal, have attracted considerable attention because of their unusual magnetic, dielectric, and luminescence properties.[1-3] Recently, the luminescence properties have been extensively studied in many ABO_3 perovskite structures (A = Sr, Ba, K, etc., B = Nb, Ti, Ta, etc.), and this has provided information on the photochemical properties of ABO_3 perovskites, such as photocatalysis, photoinduced electron-transfer dynamics, and excitation energy transport.[2-5] These ABO_3 perovskites exhibit a broad emission band with a large Stokes shift at low temperatures, whereas the luminescence is usually quenched at high temperatures and it is hard to detect at room temperature. Several mechanisms for the luminescence properties of ABO_3 perovskites have been proposed. They include the recombination of electrons trapped on the donors with holes trapped on the acceptors,[6] radiative transitions within the BO_6;[7] self-trapped excitons,[2,5] and charge-transfer vibronic excitons.[8,9] Moreover, Longo et al. have attributed the origin of the visible luminescence emission in perovskite-type compounds to the localized electronic level induced in the valence band by the symmetry.[10] The semiempirical quantum chemical method of intermediate neglect of differential overlap has been used by Grigorjeva et al. for investigating the radiative recombination of correlated (bound) self-trapped electron and hole polarons in the highly polarizable ABO_3-type matrix.[11] Orhan et al. have turned to the first-principles theory as an appropriate tool to analyze the mechanism of the luminescence behavior in disordered ABO_3 materials.[12] However, a clear understanding of the luminescence behavior of ABO_3 materials is still needed.

Among the different ABO_3 materials, $NaTaO_3$ presents a widely versatile structure, depending on growth techniques, and the structure would influence the optical properties of $NaTaO_3$.[13-15] Wiegel et al. have reported the relationship between crystal structure and energy delocalization for perovskite-type alkali tantalates.[13] The excited energy is efficiently delocalized at a bond angle of Ta−O−Ta close to 180°, while the excited energy would be localized at bond angles deviating from 180°. The luminescence of ABO_3 materials at low temperatures has been explored by numerous studies. In contrast, only a limited number of studies has reported the luminescence at room temperature. For example, De Figueiredo et al.[16] and Gu et al.[17] have observed the visible luminescence at room temperature in disordered titanate materials. The intense luminescence from zirconates and stanates at room temperature has been reported by Longo et al.[18] and Zhang et al.,[19] respectively. However, the room-temperature luminescence from tantalate compounds has not been well explored.[13,20]

In this work, we report the temperature dependence of the photoluminescence (PL) spectra of the $NaTaO_3$ species. Two different structures of $NaTaO_3$, the monoclinic and orthorhombic phases, were prepared by the sol-gel (SG) and solid-state (SS) methods, respectively. The difference between the PL spectra of the SG and SS $NaTaO_3$ is used to explore how the crystalline structure would affect the luminescence behaviors.

Experimental

Detailed processes for synthesizing $NaTaO_3$ with SG and SS methods have been reported elsewhere.[21] In brief, a solution of CH_3COONa, $TaCl_5$, and citric acid was used in the sol-gel synthesis, with the SG $NaTaO_3$ obtained after calcination at 500°C. The SS $NaTaO_3$ was obtained by calcining a mixture of Na_2CO_3 and Ta_2O_5 in air at 1200°C. In our previous report,[21] the crystalline structure of the SG and SS $NaTaO_3$ was analyzed by powder X-ray diffraction (XRD, Rigaku RINT2000). By comparing with the $NaTaO_3$ patterns documented in the powder diffraction files of the JCPDS, the SG and SS $NaTaO_3$ samples should be assigned to the monoclinic ($P2/m$ with $a = 3.8995$ Å, $b = 3.8965$ Å, and $c = 3.8995$ Å, $\alpha = \gamma = 90°$, and $\beta = 90.15°$) and orthorhombic ($Pcmn$ with $a = 5.5213$ Å, $b = 7.7952$ Å, and $c = 5.4842$ Å, and $\alpha = \beta = \gamma = 90°$) phases, respectively.

PL measurements were conducted under the excitation with a 5 mW/cm^2 of a microchip laser (266 nm). The luminescence was collected using a spectrometer (Acton SP-2150i) with a 1200 grooves/mm grating and detected using a GaAs photomultiplier tube. The PL signal obtained from the photomultiplier was analyzed using the lock-in technique and recorded in a computer. In addition, a Janis Research model CCS-150 and LakeShore model 321 temperature controller were used to measure the PL spectrum as a function of temperature. Ultraviolet-visible (UV-vis) diffuse-reflection spectra were measured for the specimens using a UV-vis spectrometer (Varian CARY 100).

Results and Discussion

Figure 1 shows the absorption and PL spectra of the $NaTaO_3$ specimens measured at 300 K, except that the PL of the SG $NaTaO_3$ was obtained at 220 K. The absorption spectrum was obtained by converting diffuse reflectance data to absorbance with the Kubelka–Munk method. From onsets of the absorption, bandgaps for the SG and SS $NaTaO_3$ were estimated to be around 4.1 and 4.0 eV, respectively.

* Electrochemical Society Active Member.
z E-mail: jacklee@mail.tnu.edu.tw

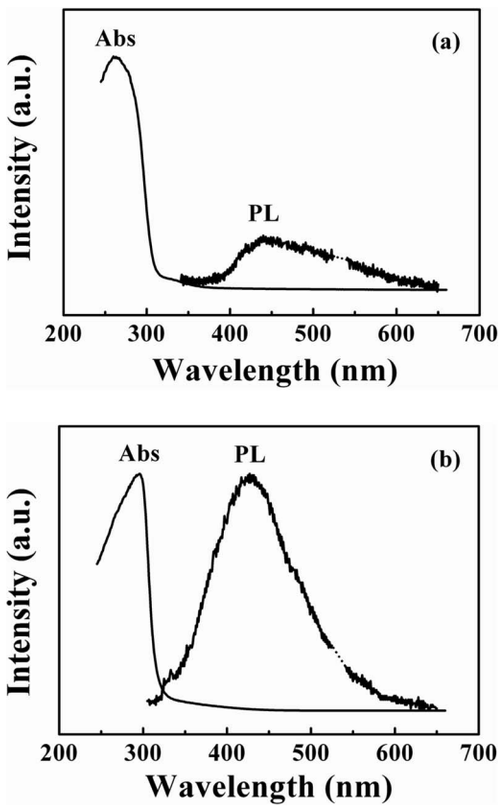

Figure 1. (a) Absorption spectra at 300 K and PL at 220 K for the SG $NaTaO_3$. (b) Absorption spectra at 300 K and PL at 300 K for the SS $NaTaO_3$. The PL spectra are amplified with the same factor for comparison.

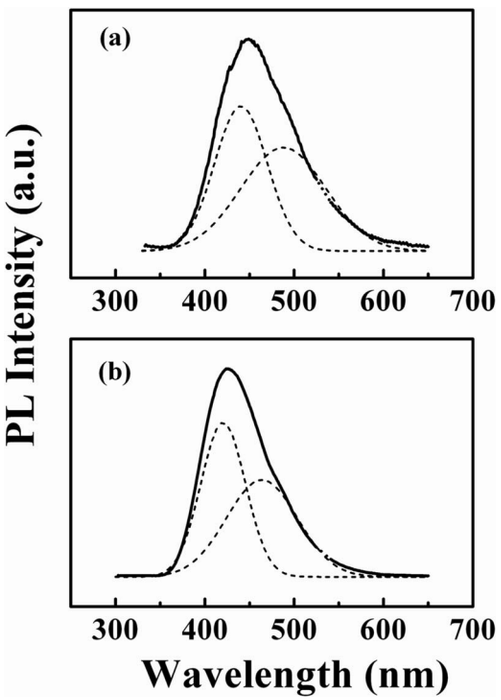

Figure 2. PL spectra at 10 K for the (a) SG $NaTaO_3$ and (b) SS $NaTaO_3$. The spectra can be decomposed into two Gaussian peaks.

The PL spectra, excluding the second-order line (533 nm) from the excitation line at 266 nm, are amplified with the same factor for comparison. Clearly, the PL intensity of the SG $NaTaO_3$ is much weaker than that of the SS $NaTaO_3$. The luminescence of the SG $NaTaO_3$ cannot be detected at temperatures above 220 K. The luminescence from the SS $NaTaO_3$ can be successfully detected at room temperature and exhibits a broad emission band centered at 427 nm with a large Stokes shift (11,420 cm^{-1}). The luminescence radiating at room temperature implies that the SS $NaTaO_3$ is favorable for optical applications.

Among the several mechanisms for discussing the origins of visible luminescence in perovskite-type tantalates ($ATaO_3$) or titanates ($ATiO_3$), the recombination of the trapped electron and hole (exciton) has been recognized as a characteristic feature of current research.[8,13] The research by Leonelli et al. indicated that the visible emission is intrinsic in origin in strontium titanate ($SrTiO_3$) and corresponds to the recombination of a self-trapped exciton (STE).[2] Recently, Vikhnin and Kapphan have demonstrated an exciton structure theoretically and experimentally in ABO_3-type materials, and they named it charge-transfer vibronic excitons (CTVE).[8,9] The CTVE is composed of a pair of an electron polaron and a hole polaron that arose from a defect-bound or self-trapped exciton, such as Ta^{4+}–O^- (Ti^{3+}–O^-) state in the TaO_6 (TiO_6) octahedron. However, the STE model should be somewhat analogous to the CTVE model, because both STE and CTVE models attribute the large Stokes shift to a strong electron-lattice interaction and exciton relaxation in ABO_3 ferroelectric oxides.[5,13]

To understand the luminescence mechanism of $NaTaO_3$, we carried out the PL analysis at 10 K for the SG and SS $NaTaO_3$. As shown in Fig. 2a and b, the SG $NaTaO_3$ has a longer wavelength in the peak position. The present study deduces that the origin of luminescence in $NaTaO_3$ is related to the electron–hole pair recombination of a localized exciton Ta^{4+}–O^- in a TaO_6 octahedron; therefore, the formation of Ta–O–Ta might play an important role in shaping the overall contour of the luminescence spectrum. The SG and SS $NaTaO_3$ have been known to be the monoclinic and orthorhombic phases, respectively. Thus, the Ta–O–Ta angle in the SG $NaTaO_3$ is close to 180°, while that in the SS $NaTaO_3$ is about 163°.[22] Wiegel et al. have reported that the M–O–M (M = Nb, Ta, Ti, etc.) angle approaching 180° would increase the amount of delocalization.[23] A larger amount of delocalization implies that an enormous number of electron–hole pairs formed by absorption of light can easily separate and migrate to active sites for photocatalytic reactions, while a few electron–hole pairs have the probability to recombine at the lower energy state. Therefore, the PL of SG $NaTaO_3$ exhibits the weak and longer wavelength.[13,23] In other words, the emission could originate from a great quantity of localized states trapping the migration excitons. The difference between the luminescence spectra of the SG and SS $NaTaO_3$ is in accordance with the above argument for the origin of luminescence. Hence, the Ta–O–Ta angle deviating from 180° in the SS $NaTaO_3$ is the main cause for the high luminescence efficiency.

Figures 3 and 4 illustrate the PL spectra at different temperatures for the SG and SS $NaTaO_3$, respectively. It is obvious that the PL behavior significantly depends on temperature. Both the PL intensity of the SG and SS $NaTaO_3$ decrease significantly with increasing temperature. In addition, the peak position as a function of temperature is depicted in the insets of Fig. 3 and 4. Both insets exhibit similar behavior, showing that the peak position of the emission band shifts to longer wavelength with increasing temperature and then shifts to shorter wavelength above 140 K. However, the peak-shifting behavior is inconsistent with the temperature dependence of the electronic states in bulk semiconductors.[24,25]

To discuss how the peak position varies as a function of temperature, the luminescence spectra are decomposed into two peaks and fitted to a symmetric Gaussian function. Figure 2 shows the typical peak-resolution results for the luminescence at 10 K, showing that two Gaussian curves constitute the overall luminescence of the

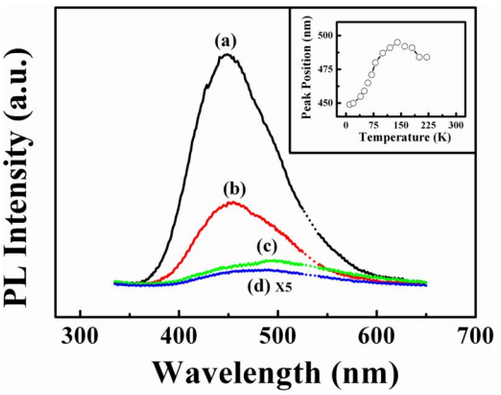

Figure 3. (Color online) PL spectra of the SG $NaTaO_3$ at different temperatures: (a) 10, (b) 40, (c) 140, and (d) 220 K. The inset shows the variation of the peak position with temperature.

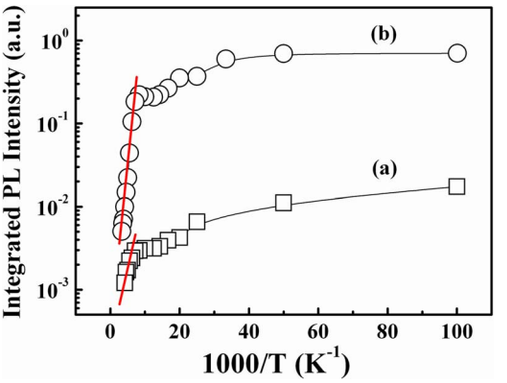

Figure 5. (Color online) Temperature dependence of the integrated PL intensity for (a) SG $NaTaO_3$ and (b) SS $NaTaO_3$.

$NaTaO_3$ specimens. Two emission bands for the SG $NaTaO_3$ are obtained with peak positions at around 440 and 488 nm, which are in agreement with Ref. 13. The peak positions from the decomposition for the SS $NaTaO_3$ are about 420 and 465 nm. In the low-temperature regime (<140 K), it should be the case that the intensity decrease of the short-wavelength peak with temperature was more prominent, thus leading to the redshift of the overall luminescence. The phenomenon is quite similar to a report by Yamaichi et al.[6,26] As the temperature increases, the luminescence spectrum shifts toward higher energy because the intensity of the shorter emission wavelength increases. However, clear mechanisms for the two distinct emissions have not been understood yet, and those could be clarified by time-resolved PL in the future.

The integrated PL intensity (I) vs temperature (T) is plotted in Fig. 5 for the SG and SS $NaTaO_3$. The experimental data can be described by[27,28]

$$I(T) = \frac{I_0}{1 + C\ \exp(-E_A/k_B T)} \qquad [1]$$

where C is a constant, I_0 is the PL intensity at 0 K, E_A is the thermal activation energy, and k_B is the Boltzmann constant. By plotting ln I against $1/T$ in the high-temperature regime, the value of E_A can be calculated from the slope of the linear relationship. The thermal activation energy derived from Eq. 1 for the SG and SS $NaTaO_3$ is thus determined to be 23 and 86 meV, respectively. Huang et al. have reported that the strong exciton localization would lead to the larger thermal activation energy.[28] The large thermal activation energy could efficiently prevent carriers from thermal quenching and ensures strong emission up to room temperature,[28,29] which explains the much stronger PL of the SS $NaTaO_3$.

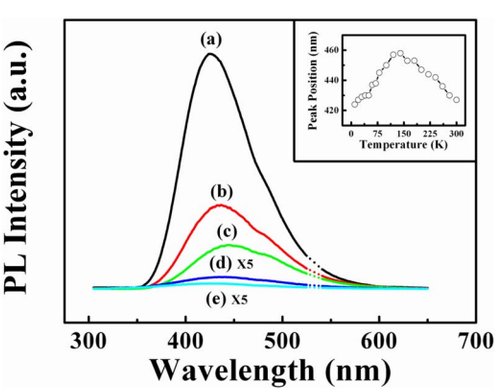

Figure 4. (Color online) PL spectra of the SS $NaTaO_3$ at different temperatures: (a) 10, (b) 60, (c) 120, (d) 240, and (e) 300 K. The inset shows the variation of the peak position with temperature.

Conclusion

In summary, the present work has investigated the temperature dependence of PL of the SG and SS $NaTaO_3$. The visible and intense PL of the SS $NaTaO_3$ with orthorhombic structure measured at room temperature indicates that the SS $NaTaO_3$ is a promising material for future optical applications. A comparison of temperature-dependent luminescence between the SG and SS $NaTaO_3$ was also discussed. This paper demonstrates that the origin of luminescence of $NaTaO_3$ is attributed to the localized exciton Ta^{4+}–O^- in a TaO_6 octahedron, and the formation of a Ta–O–Ta angle results in PL behavior with temperature dependence.

Acknowledgments

This research was supported by the National Science Council of Taiwan through projects NSC 96-2112-M-236-001-MY3 and NSC 95-2221-E-006-408-MY3.

Tungnan University assisted in meeting the publication costs of this article.

References

1. T. Feng, *Phys. Rev. B*, **25**, 627 (1982).
2. R. Leonelli and J. L. Brebner, *Phys. Rev. B*, **33**, 8649 (1986).
3. L. Grigorjeva, D. Millers, A. I. Popov, E. A. Kotomin, and E. S. Polzik, *J. Lumin.*, **72–74**, 672 (1997).
4. V. V. Laguta, M. D. Glinchuk, I. P. Bykov, A. Cremona, P. Galinetto, E. Giulotto, L. Jastrabik, and J. Rosa, *J. Appl. Phys.*, **93**, 6056 (2003).
5. W. F. Zhang, J. Tang, and J. Ye, *Chem. Phys. Lett.*, **418**, 174 (2006).
6. E. Yamaichi, K. Watanabe, K. Imamiya, and K. Ohi, *J. Phys. Soc. Jpn.*, **56**, 1890 (1987).
7. H. Liu, R. C. Powell, and L. A. Boatner, *J. Appl. Phys.*, **70**, 20 (1991).
8. V. S. Vikhnin and S. Kapphan, *Phys. Solid State*, **40**, 834 (1998).
9. V. S. Vikhnin, *Phys. Solid State*, **47**, 1548 (2005).
10. E. Longo, E. Orhan, F. M. Pontes, C. D. Pinheiro, E. R. Leite, J. A. Varela, P. S. Pizani, T. M. Boschi, F. Lanciotti, Jr., A. Beltrán, et al., *Phys. Rev. B*, **69**, 125115 (2004).
11. L. Grigorjeva, D. K. Millers, V. Pankratov, R. T. Williams, R. I. Eglitis, E. A. Kotomin, and G. Borstel, *Solid State Commun.*, **129**, 691 (2004).
12. E. Orhan, J. A. Varela, A. Zenatti, M. F. C. Gurgel, F. M. Pontes, E. R. Leite, E. Longo, P. S. Pizani, A. Beltràn, and J. Andrès, *Phys. Rev. B*, **71**, 085113 (2005).
13. M. Wiegel, M. H. J. Emond, E. R. Stobbe, and G. Blasse, *J. Phys. Chem. Solids*, **55**, 773 (1994).
14. H. Kato and A. Kudo, *Catal. Lett.*, **58**, 153 (1999).
15. Y. X. Wang, W. L. Zhong, C. L. Wang, and P. L. Zhang, *Solid State Commun.*, **120**, 137 (2001).
16. A. T. de Figueiredo, V. M. Longo, S. de Lazaro, V. R. Mastelaro, F. S. De Vicente, A. C. Hernandes, M. S. Li, J. A. Varela, and E. Longo, *J. Lumin.*, **126**, 403 (2007).
17. H. Gu, Y. Hu, J. You, Z. Hu, Y. Yuan, and T. Zhang, *J. Appl. Phys.*, **101**, 024319 (2007).
18. V. M. Longo, L. S. Cavalcante, A. T. de Figueiredo, L. P. S. Santos, E. Longo, J. A. Varela, J. R. Sambrano, C. A. Paskocimas, F. S. De Vicente, and A. C. Hernandes, *Appl. Phys. Lett.*, **90**, 091906 (2007).

19. W. Zhang, J. Tang, and J. Ye, *J. Mater. Res.*, **22**, 1859 (2007).
20. I. Katayama and K. Tanaka, *J. Phys. Soc. Jpn.*, **75**, 064713 (2006).
21. W. H. Lin, C. Cheng, C. C. Hu, and H. Teng, *Appl. Phys. Lett.*, **89**, 211904 (2006).
22. H. Kato and A. Kudo, *J. Phys. Chem. B*, **105**, 4285 (2001).
23. M. Wiegel, M. Hamoumi, and G. Blasse, *Mater. Chem. Phys.*, **36**, 289 (1994).
24. Y. P. Varshni, *Physica*, **34**, 149 (1967).
25. P. Lautenschlager, M. Garriga, S. Logothetidis, and M. Cardona, *Phys. Rev. B*, **35**, 9174 (1987).
26. E. Yamaichi, K. Watanabe, and K. Ohi, *J. Phys. Soc. Jpn.*, **57**, 2201 (1988).
27. S. Mochizuki, F. Fujishiro, and S. Minami, *J. Phys.: Condens. Matter*, **17**, 923 (2005).
28. J. S. Huang, Z. Chen, X. D. Luo, Z. Y. Xu, and W. K. Ge, *J. Cryst. Growth*, **260**, 13 (2004).
29. Y. Zhang, B. Lin, X. Sun, and Z. Fu, *Appl. Phys. Lett.*, **86**, 131910 (2005).